

# A Fault Tolerant Control Structure for an Induction Motor Drive System

DOI 10.7305/automatika.2017.02.1642  
UDK [681.516.7.037.09:681.586-531.6]:621.313.333

Original scientific paper

In this paper the Fault Tolerant (FT) vector controlled induction motor drive system is described and tested in various drive conditions. The influence of the rotor speed sensor faults on the properties of the analyzed drive are tested. Faults detection algorithms, based on different algorithms are developed and described. The results of the simulation carried out using the MATLAB/SimPowerSystem software are verified in experimental tests in MicroLabBox DS1202, in a wide range of motor speed changes. The proposed detection algorithms can be successfully applied in the Fault Tolerant Drive Systems (FTDS).

**Key words:** Fault detection, Fault tolerant drive, Speed estimator, Speed sensor faults

**Struktura upravljanja indukcijskog motora otporna na kvarove.** U ovom radu opisan je sustav za vektorsko upravljanje indukcijskim motorom otporno na kvarove. Sustav je testiran u različitim uvjetima rada. Testiran je utjecaj kvarova rotorskog senzora brzine na svojstva analiziranog sustava. Razvijeni su i opisani različiti algoritmi za detekciju kvarova. Simulacijski rezultati u MATLAB/SimPowerSystem provjereni su eksperimentalno u MicroLabBox DS1202 za široki raspon promjena brzine motora. Predloženi algoritam se može uspješno primjeniti u sustavima upravljanja otpornima na kvarove.

**Ključne riječi:** detekcija kvara, upravljanje otporno na kvarove, estimacija brzine, kvarovi senzora brzine

## 1 INTRODUCTION

To achieve the proper work of the modern vector controlled induction motor drive system the mechanical and electrical variables sensors are necessary [1]. Some signals, used in the internal control structure of the drive system, (like stator and/or rotor flux, electromagnetic torque, rotor speed) can be estimated by different simulators, observers, Kalman Filters [1–4] or neural networks [1]. Those estimation systems and control algorithms cannot work stably when the sensors are broken [5]. Elements which can be broken in an electrical drive system are presented in Fig. 1.

In various articles, problems connected with the faulted operation of the system with mechanical faults of the drive are presented and described. The main problem in this system is rotor and stator fault identification and compensation [1, 3, 6, 7]. Another problem reported in the literature is associated with a damage of the semiconductor components of the AC and DC system [8, 9]. Different techniques and methodologies of identification of these faults are presented. Some are based on redundancy of the power electronics, others are based on the adaptation of the drive system to the current drive conditions [4, 9].

In the electrical drive system current and voltage sensors are necessary for the proper work of vector control algorithms [10, 11]. These sensors are very sensitive and can be broken [5, 12, 13]. A drive system and estimation techniques can work stably without information from a stator voltage sensor, but cannot work properly without signals from stator current sensors [5, 14, 15]. Those signals are used for state variable reconstruction [11, 16].

One of the most important signals used in the electrical drive system is the rotor speed. Mechanical sensors can be used to measure this variable [5]. Those elements are very sensitive to the current drive and weather conditions [15] and they can be destroyed. Some types of the drive can work stably without information about this signal [16] but others cannot be stable. The topology of the drive must be changed if the speed sensor is broken [5, 15].

The advanced control structures of Induction Motor (IM) drives should be equipped with diagnostic features to prevent damages and sudden switch-offs of complex industrial installations [5, 9, 17]. Thus the incipient fault detection has recently become one of the basic requirements for modern IM drive systems [4, 5, 12, 13, 17, 18].

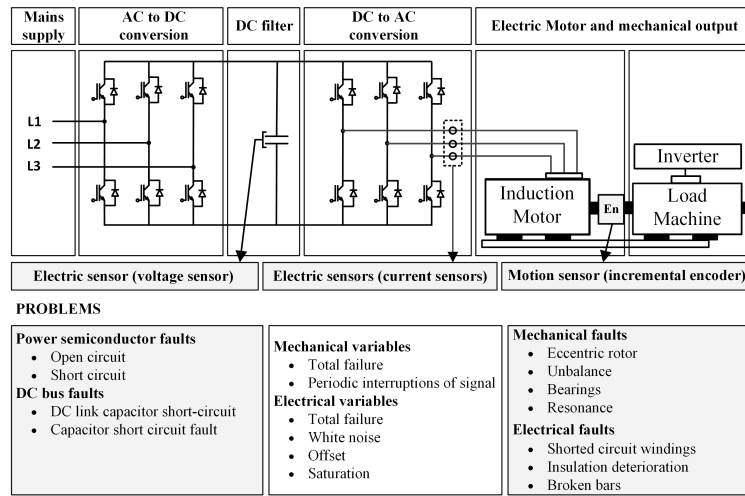


Fig. 1: The faulted conditions in VSD [10]

During the last few years, fault tolerant control systems (FTCS) became a very active field for many research groups [4, 5, 18]. The FTC aims to ensure the continuous system functionality, even after fault occurrence. Therefore, FTC should be able to detect and identify faults and to cancel their effects or to attenuate them to an acceptable level [13, 18]. FTC systems possess the ability to detect component failures automatically. They are capable of maintaining overall system stability and acceptable performance in the event of such failures. In other words, a closed-loop control system, which can tolerate component malfunctions while maintaining desirable performance and stability properties, is said to be a fault tolerant control system. The general scheme of the FTC system is pre-

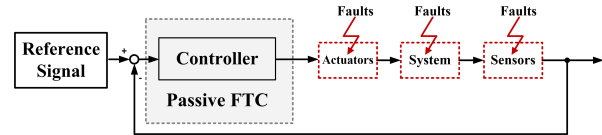


Fig. 3: The scheme of passive FTCS

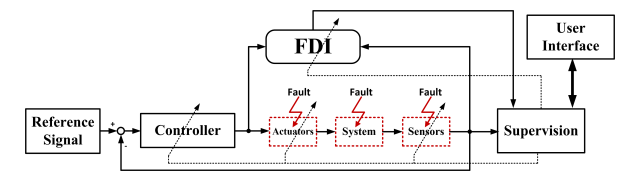


Fig. 2: The scheme of FTCS with supervision subsystem

sented in Fig. 2. The FDI (Fault Detection and Isolation) unit is responsible for providing the supervision system with information about the location and severity of any faults [19, 20]. Based on the system inputs, outputs and information from the FDI unit, the supervision system will reconfigure the sensor set and/or actuators to isolate faults, and tune or adapt the controller to accommodate the fault effects.

The Fault-Tolerant Control Systems - FTCS can be classified as passive and active systems [5, 19, 20]. The first group is designed to provide the optimum performance of

a faulted drive. It is not necessary to identify the type of the fault [5]. The adaptive and predictive [21] control drives [12, 18] belong to this group. The scheme of this system is presented in Fig. 3. These systems use control techniques to provide closed loop control system insensitivity to certain failures, the faulty process continues operation with the same structure and parameters of the controller. The systems have an advantage over conventional control structures, they improve the efficiency, performance and also they are less complex [5, 19]. Active

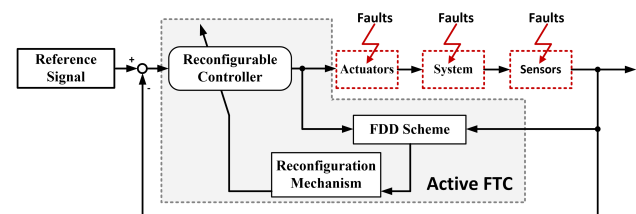


Fig. 4: The scheme of active FTCS

systems use detectors or observers [12] to identify a failure condition. The main goal is stable operation of the drive, which can be obtained by additional sensors, estimators, control loops or redundant elements [4, 12].

The scheme of AFTC system is presented on the Fig. 4.

The main goal of this paper is to demonstrate a simple

speed sensor fault detection algorithm for the vector control (DTC-SVM and DFOC) of an induction motor drive system, based on an active detection system [18]. The proposed systems guarantee stable operation of the drive during faulted conditions [4, 12]. Those systems are based on simple signals from the internal control structure and the estimated speed and rotor flux. The diagnostic methods are analyzed and tested in various drive operation conditions. The MRAS type speed estimator is applied as a redundant system to the motor speed reconstruction. Simulations and experimental results of the proposed Fault Tolerant Control are presented.

## 2 SPEED SENSOR FAULTS ANALYSIS

Speed sensor faults can be determined by the equation [5, 11, 15]:

$$\omega_m^{enc} = (1 - \gamma)\omega_m, \tag{1}$$

where  $\omega_m^{enc}$  - measured rotor speed,  $\omega_m$  - real rotor speed,  $\gamma$  - constant coefficient.

For different values of the coefficient  $\gamma$ , the measured rotor speed can be:

- a) intermittent - partial damage of the speed sensor consisting in a partial failure of individual pulses from the encoder -  $-1 < \gamma < 1$ ;
- b) intermittent - partial damage of the speed sensor consisting in a cyclic interruption of specific pulses from the encoder -  $\gamma = [0, 1]$ ;
- c) zero - total failure of the speed sensor -  $\gamma = 1$ ;
- d) with offset -  $\gamma = const \in (-1, 1)$ ;

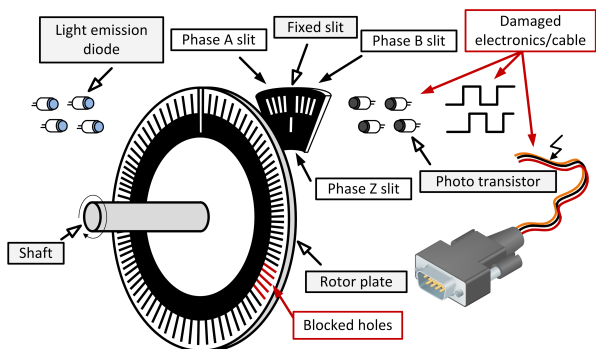


Fig. 5: The scheme of the simplified structure of incremental encoder

The number of pulses of the sensor can be limited as a result of blocking holes in sensor's ring and the periodic interruptions of the measurement signal occur due to the damage of the electronics or connecting cables (Fig. 5).

On the basis of reports in the literature it can be observed that the effects of a speed sensor failure in the

vector-controlled induction motor drives are most visible in the error between the measured and estimated speed and in the estimated electromagnetic torque (or stator current components) [11, 15]. In the vector-controlled IM drives,

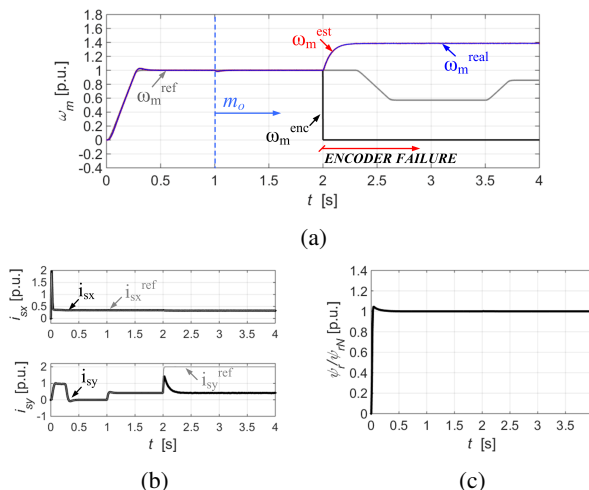


Fig. 6: Transients of the measured and estimated speed, stator current components, rotor flux vector for a total failure of the speed sensor in a DFOC structure

the symptoms of the rotor speed sensor faults can be observed in the internal state variables of the motor and control structure as: stator current components, rotor (or stator) flux magnitude, control voltages [5]. So monitoring these signals can be useful from the diagnostic point of view.

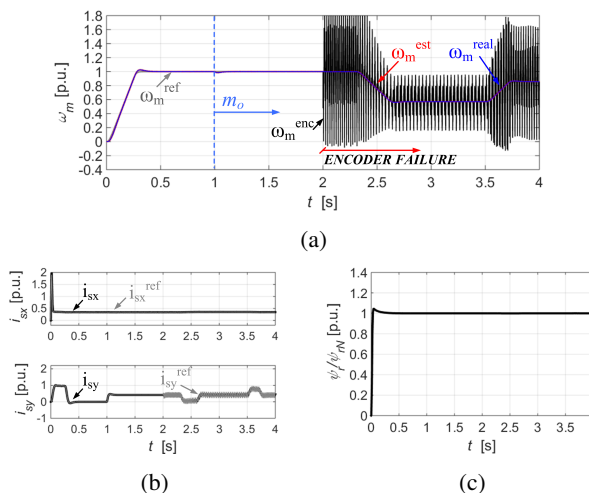


Fig. 7: Transients of the measured and estimated speed, stator current components, rotor flux vector for a partial loss of individual pulses of the speed sensor in a DFOC structure

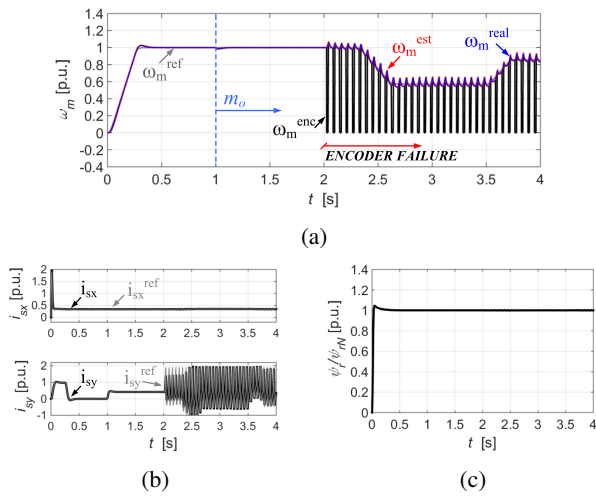


Fig. 8: Transients of the measured and estimated speed, stator current components, rotor flux vector for a cyclic interruption of specific pulses from the encoder in a DFOC structure

In Fig. 6 – Fig. 8 the influence of the incremental encoder faults on the properties of the DFOC structure are presented, they were obtained by modeling different speed sensor faults (eq. 1). It was assumed that the damage is a complete interruption of the feedback loop from the speed sensor (Fig. 6), a loss of individual pulses (Fig. 7) or a cyclic loss of these pulses (Fig. 8). The drive is started from zero to the nominal speed (at  $t = 1s$  drive is loaded  $m_o = 0.5m_{oN}$ ).

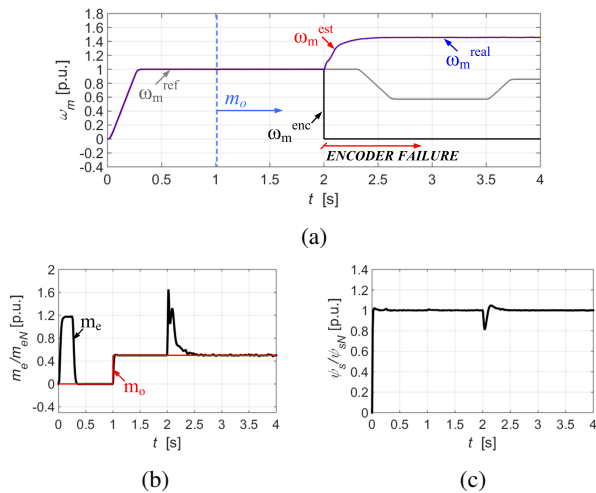


Fig. 9: Transients of the measured and estimated speed, electromagnetic torque, stator flux vector for a total failure of the speed sensor in a DTC-SVM structure

Similar tests are presented for the DTC-SVM algorithm

(Fig. 9 – Fig. 11).

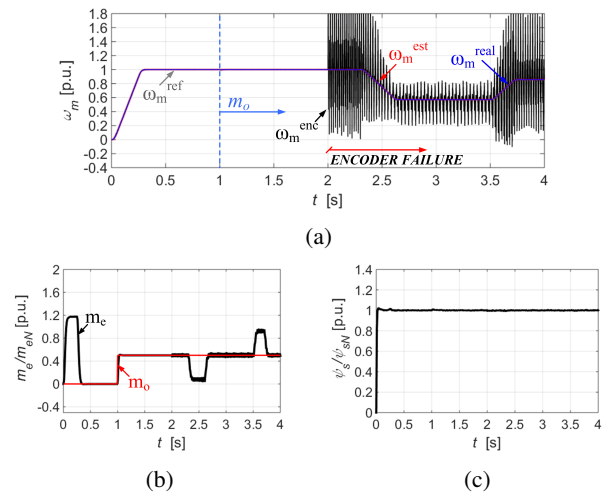


Fig. 10: Transients of the measured and estimated speed, electromagnetic torque, stator flux vector for a partial loss of individual pulses of the speed sensor in a DTC-SVM structure

The speed sensor fault occurred at  $t = 2s$ . It is visible that after the speed sensor faults in the DFOC algorithm (the total failure of the encoder Fig. 6), the partial failure of individual pulses of the encoder Fig. 7) or a cyclic interruption of specific pulses from the encoder Fig. 8)), abnormal behaviors of the system are observed. In this control algorithm reference signals are limited (current  $i_{sy}$  limit is set to 2 in [p. u.]).

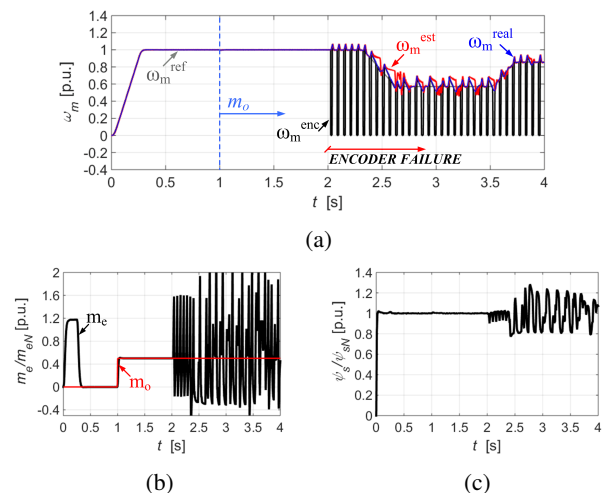


Fig. 11: Transients of the measured and estimated speed, electromagnetic torque, stator flux vector for a cyclic interruption of specific pulses from the encoder in a DTC-SVM structure

In the total failure of the speed sensor, the real and estimated speed of the drive increase (Fig. 6 and Fig. 9). The interruption of the speed loop caused also the increase in the electromagnetic torque.

In a partial loss of individual pulses (Fig. 7 and Fig. 10) and a cyclic interruption of specific pulses of the speed sensor (Fig. 8 and Fig. 11) speed oscillation is visible. In both cases drives are stable. After speed sensor faults, the stator current component  $i_{sy}$  is not constant. Oscillations on this variable are visible, the amplitude depends on the fault type. The worst behaviour is observed for a cyclic interruption of specific pulses. A similar situation is observed on the electromagnetic torque in a DTC-SVM control system (Fig. 11).

### 3 SPEED SENSOR FAULT DETECTION

In this chapter selected methods of the speed sensor faults detection, for DFOC and DTC-SVM algorithms, based on the algorithmic method and neural networks, are presented. These methods are based on the signal taken from the internal control loop.

For the Direct Field Oriented Control structure the stator current components ( $i_{sy}$  and  $i_{sy}^{ref}$ ), and the rotor speed (measured and estimated), for the DTC-SVM electromagnetic torque and an estimated stator flux are used.

In both cases, the estimated rotor speed must be used in the diagnostic process. For rotor speed estimation the MRAS<sup>CC</sup> estimator is used. This system was presented in detail in [11]. This estimator is based on two well-known simulators (a voltage model and current model of the rotor flux) transformed to the stator current estimator and to the rotor flux estimator based on a current model.

In the basis control structure the rotor flux can be calculated from the equation in [p. u.] system [11]:

$$\frac{d}{dt} \Psi_r^i = \left[ \frac{r_r}{x_r} (x_m \mathbf{i}_s - \Psi_r^i) + j\omega_m \Psi_r^i \right] \frac{1}{T_N} \quad (2)$$

The current estimator used in MRAS<sup>CC</sup> is obtained using the equation:

$$\begin{aligned} \frac{d}{dt} \mathbf{i}_s^e = & \frac{r_r x_m^2 + x_r^2 r_s}{\sigma T_N x_s x_r^2} \mathbf{i}_s^e + \frac{x_m r_r}{\sigma T_N x_s x_r^2} \Psi_r^i + \\ & + \frac{1}{\sigma T_N x_s} \mathbf{u}_s - j\omega_m^e \frac{x_m}{\sigma T_N x_s x_r} \Psi_r^i \end{aligned} \quad (3)$$

where  $\omega_m^e$  - estimated rotor angular speed,  $r_s, r_r, x_s, x_r, x_m$  - stator and rotor resistances, stator and rotor leakage reactances, mutual reactance,  $\mathbf{u}_s, \mathbf{i}_s^e, \Psi_r^i$  - stator voltage, the estimated stator current and rotor flux vectors,  $\sigma = 1 - x_m^2/x_s x_r, T_N = 1/2\pi f_{sN}$  respectively.

Both the stator current model (3) and the rotor flux model (2) are adjusted by the estimated rotor speed [11]:

$$\begin{aligned} \omega_m^e = & K_P (e_{i_{s\alpha}} \Psi_{r\beta}^i - e_{i_{s\beta}} \Psi_{r\alpha}^i) + \\ & + K_I \int (e_{i_{s\alpha}} \Psi_{r\beta}^i - e_{i_{s\beta}} \Psi_{r\alpha}^i) dt \end{aligned} \quad (4)$$

where  $e_{i_{s\alpha,\beta}} = i_{s\alpha,\beta} - i_{s\alpha,\beta}^e$  - error between the estimated and measured stator current.

The detection algorithms for DFOC and for DTC - SVM consist of four stages (Fig. 12 - 13). At the first stage the measured and estimated (or reference and estimated) signals are compared and checked. At the second stage signals are compared with the limits.

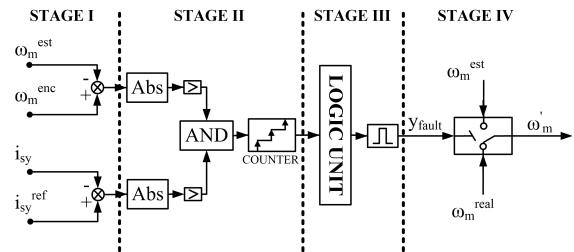


Fig. 12: The block diagram of the speed sensor fault detector for the DFOC algorithm

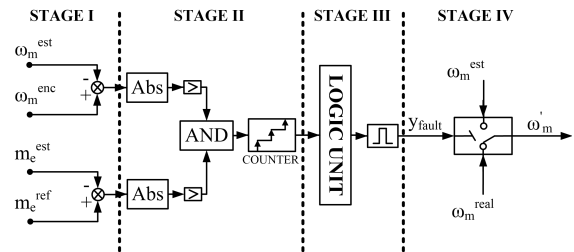


Fig. 13: The block diagram of the speed sensor fault detector for the DTC-SVM algorithm

If the differences between those signals are bigger than the assumed limit (chosen arbitrarily), a simple logic algorithm (stage 3) detects the speed sensor fault in the following way:

For the DFOC algorithm:

$$\begin{cases} |(\omega_m - \omega_m^e)| \geq \epsilon_1 \\ |(i_{sy}^{ref} - i_{sy})| \geq \epsilon_2 \end{cases} \Rightarrow \omega_m^e \text{ ELSE } \omega_m \quad (5)$$

for the DTC-SVM algorithm:

$$\begin{cases} |(\omega_m - \omega_m^e)| \geq \epsilon_3 \\ |(m_e^{ref} - m_e)| \geq \epsilon_4 \end{cases} \Rightarrow \omega_m^e \text{ ELSE } \omega_m \quad (6)$$

where  $\epsilon_1, \epsilon_3 = 0,02 + 0,1 \cdot |\omega_m^{ref}|$  - maximum speed error,  $\epsilon_4 = \zeta \cdot |m_N| \cdot |\omega_m^{ref}|$ ,  $\zeta \geq 2$  - maximum torque error,  $\epsilon_2 = 2,0 \cdot |\omega_m^{ref}|$  - maximum current error.

The limit  $\epsilon$  depends on the current value of the reference speed. This solution provides stable operation of the detector during induction motor parameter variations and wrong speed and/or flux estimation. The final stage (stage 4) of the detector consists in the isolation of the fault by switching to the speed estimator (MRAS<sup>CC</sup> [11]) when a failure has been confirmed. When the failure is eliminated, the detector can switch the control back to the sensor mode if it is necessary.

The main problem in these algorithms, is the correct choice of the maximum speed error and the maximum stator current (or torque) error. It is well known that all rotor speed observers are more or less sensitive to the induction motor parameter variations. In the case of incorrect identification of those parameters, the rotor speed can be estimated with a steady state error. The first part of the detector (based on the speed error) cannot properly detect speed sensor faults. The second part of this detector (based on the stator current error) guarantees proper operation for this situation.

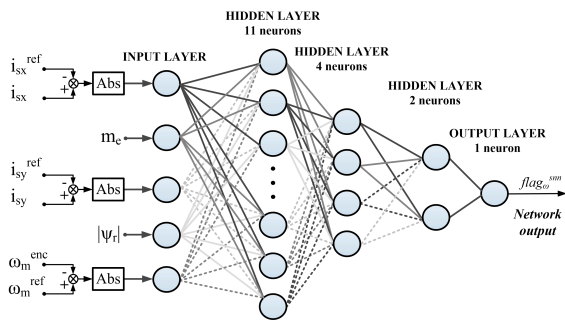


Fig. 14: The block diagram of the speed sensor fault detector based on a neural network for the DFOC algorithm

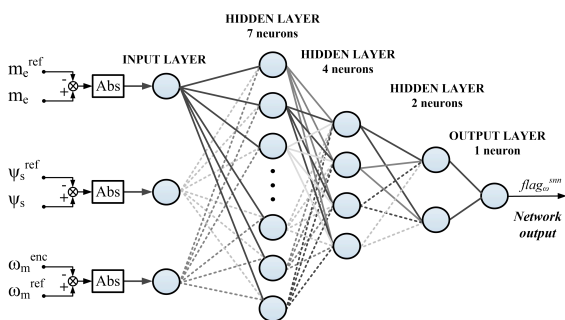


Fig. 15: The block diagram of the speed sensor fault detector based on a neural network for the DTC-SVM algorithm

Artificial intelligence can be used for rotor speed sensor faults [22, 23]. The detectors presented in Fig. 14 and Fig.

15 are based on an artificial neural network with three hidden layers in the configuration 5-11-4-2-1 (for the DFOC algorithm) and 3-7-4-2-1 (for the DTC-SVM algorithm). In the proposed systems neurons with nonlinear activation functions were used. The hidden layers consist of 17 (for the DFOC algorithm) or 13 (for the DTC-SVM algorithm) neurons, and the output layer of 1 neuron.

On the output of the NN detector there is the signal connected with the failures. Designed neural networks were trained by the Levenberg-Marquardt algorithm, which is one of the most effective ways of teaching one-way neural networks [2]. It combines the convergence of the Gauss-Newton algorithm near minimum and the method of gradient descent for a distance greater than the minimum.

The Levenberg-Marquardt (L-M) algorithm performs a compromise learning strategy between the linear model and gradient method approach in each iteration. Moving the point of seeking the optimum weight is acceptable only if it leads to a reduction of the error [24]. The Levenberg-Marquardt algorithm is a modification of the Gauss-Newton algorithm, where the minimization error  $p(\mathbf{W}(k))$  is obtained using the equation [24]:

$$p(\mathbf{W}(k)) = -[\nabla^2 \mathbf{E}(\mathbf{W}(k))]^{-1} \nabla \mathbf{E}(\mathbf{W}(k)) \quad (7)$$

In the L-M method, the exact value of Hessian is replaced by the approximated value, determined on the basis of the information contained in the gradient with emphasis on the adjusting coefficient [24]. Thus, the gradient vector and the approximated Hessian matrix corresponding to objective function are defined as [24]:

$$\nabla \mathbf{E}(\mathbf{W}(k)) = \mathbf{J}^T(\mathbf{W}(k)) \epsilon(\mathbf{W}(k)) \quad (8)$$

$$\nabla^2 \mathbf{E}(\mathbf{W}(k)) = \mathbf{J}^T(\mathbf{W}(k)) \mathbf{J}(\mathbf{W}(k)) + \mathbf{S}(\mathbf{W}(k)) \quad (9)$$

where:  $\mathbf{J}(\mathbf{W}(k))$  is the Jacobian - the matrix of first partial derivatives of the error of each sample in individual neurons of the last layer with respect to all the weights in the network, and  $\epsilon(\mathbf{W}(k))$  is the error vector for each sample in each neuron in the last layer of the network. In the Gauss-Newton method the value of the  $\mathbf{S}(\mathbf{W}(k))$  in the formula (7) is assumed to be close to zero. In the L-M algorithm it is presented as follows [24]:

$$\mathbf{S}(\mathbf{W}(k)) \approx \mu \mathbf{I} \quad (10)$$

where:  $\mu$  is the adjusting coefficient. After a modification of the equation (8) the correction of the weights in the Levenberg-Marquardt algorithm takes the form [24]:

$$\mathbf{W}(k+1) = \mathbf{W}(k) + -[\mathbf{J}^T(\mathbf{W}(k)) \mathbf{J}(\mathbf{W}(k)) + \mu \mathbf{I}]^{-1} \nabla \mathbf{E}(\mathbf{W}(k)) \quad (11)$$

The effectiveness of this algorithm determines the appropriate selection of the coefficient  $\mu$  [24]. The large initial value of this factor can be reduced in the process of optimization and reach zero value in solution close to optimum. During the learning process the reference speed value was changed in the vector controlled systems. At first, the drive runs at rated speed which was reduced at appropriate time points. During the drive operation the total interruption of the speed sensor loop occurred.

**4 FAULT TOLERANT CONTROL SYSTEM ANALYSIS**

In this part of the paper, the selected experimental results of the Fault Tolerant induction motor drive system are presented.

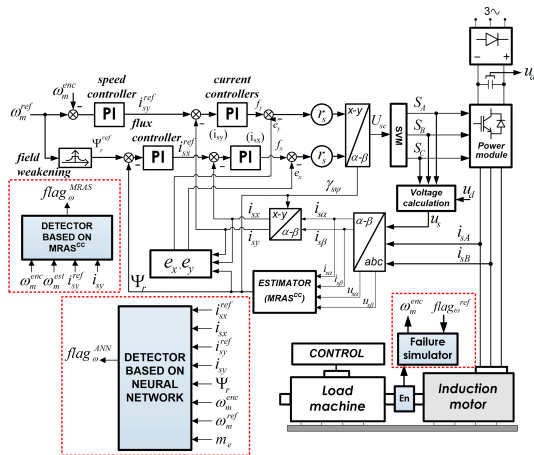


Fig. 16: The scheme of the DFOC algorithm with the diagnostic system

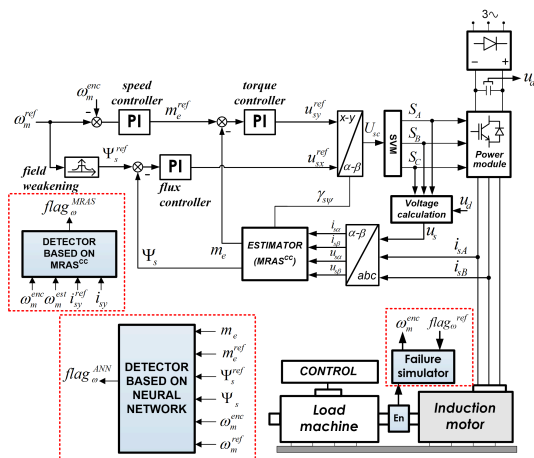


Fig. 17: The scheme of the DTC-SVM algorithm with the diagnostic system

A general scheme of the drive systems controlled by the DFOC and DTC-SVM algorithms are presented in Fig. 16 and Fig. 17, respectively. Experimental tests were conducted using a laboratory set-up consisting of 1.1 kW IM, SVM voltage inverter, an incremental encoder to measure the angular velocity (5000 imp./r). The control, detection and speed estimation algorithms were implemented using the Micro Lab Box DS1202 card. The Fault Tolerant Control (FT-DFOC and FT-DTC-SVM) drives were tested for different speeds. Two types of detectors were tested.

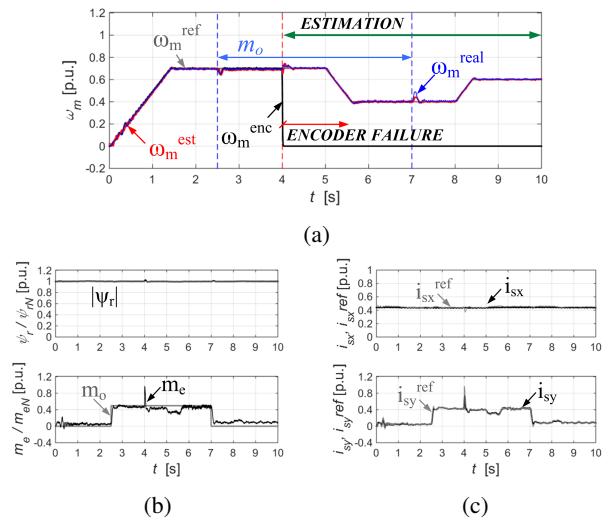


Fig. 18: Faulted operations of the DFOC drive system: measured, estimated and reference speeds (a), electromagnetic torque, rotor flux vector (b), stator currents (c) for the failure of the encoder (experimental results)  $m_o=0.5m_{oN}$  (algorithmic detector)

In Fig. 18 the DFOC algorithm analysis during the faulted operation is presented. The drive is started from zero speed to the 70% of the nominal value. After  $t=2.5s$  the drive is loaded ( $m_o=0.5m_{oN}$ ). At  $t=4s$  the rotor speed sensor is broken. After this time the detection algorithm is activated and the systems are changed to the full speed sensorless mode with the MRAS<sup>CC</sup> estimator. During the topology changes (after sensor fault detection) a small overshoot on the state variables is visible.

In Fig. 19 the experimental results of the vector controlled drive system (DFOC) with a neural network based detector are presented. The test was performed for the same conditions as the algorithmic detection system.

During topology changes the overshoot is smaller for the system with neural network based detector than for the system with the algorithmic detector (Fig. 21 and Fig. 22). System based on NN detect sensor faults faster than simple algorithmic method. In all the tested situations, the

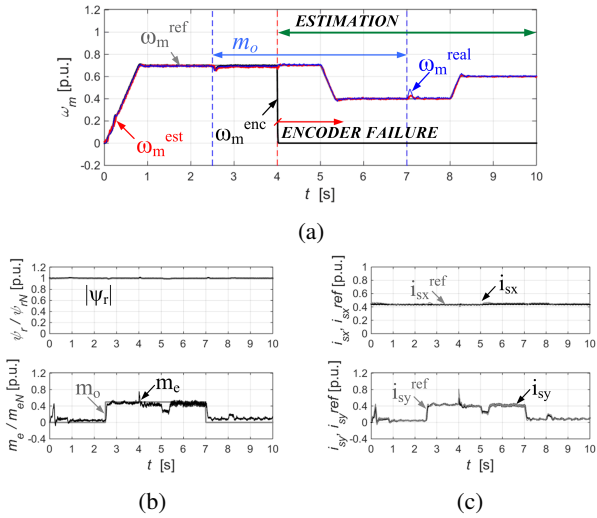


Fig. 19: Faulted operations of the DFOC drive system: measured, estimated and reference speeds (a), electromagnetic torque, rotor flux vector (b), stator currents (c) for the failure of the encoder (experimental results)  $m_o=0.5m_{oN}$  (neural network based detector)

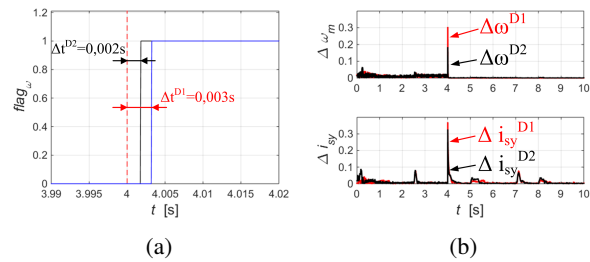


Fig. 20: Detection time and current and speed errors for system with algorithmic (D1) and the neural network (D2) based detector

fault was detected after approximately  $t=0.001s$ , therefore, the reaction of drive system to a damage was practically negligible. After the speed sensor fault detection, the drive system is switched to the full sensorless topology.

For the estimated speed, small oscillations, typical to the estimated signal, are visible (overshoot for system with neural network detector is smaller than for the algorithmic system).

### 5 CONCLUSION

In the paper the speed sensor fault detection algorithms for a vector controlled induction motor drive system was tested. Algorithmic and neural network based detectors were tested in the DFOC and DTC-SVM algorithms. Both systems can detect all types of the speed sensor fault. The

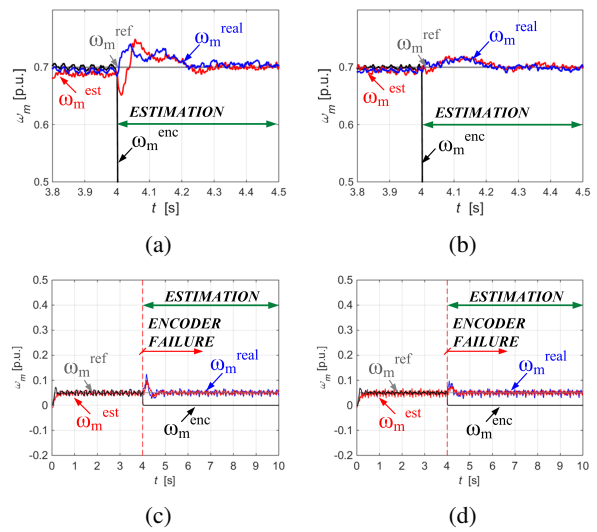


Fig. 21: Faulted operations of the DFOC drive system during topology changes (experimental results)  $m_o = 0, 5m_{oN}$  (algorithmic detector (a, c), the neural network based detector (b, d)) for 70% (a, b) and 5% (c, d) of the nominal speed

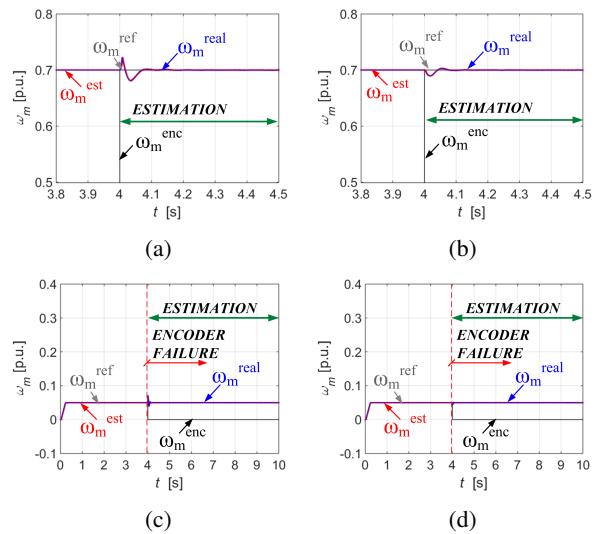


Fig. 22: Faulted operations of the DTC-SVM drive system during topology changes (simulation results)  $m_o = 0, 5m_{oN}$  (algorithmic detector (a, c), neural network based detector (b, d)) for 70% (a, b) and 5% (c, d) of the nominal speed

neural network detector is much faster than the classical solution based on simple equations. For both control structures (DFOC and DTC-SVM) the speed sensor fault is detected very fast, the systems are stable during topology changes. The main advantage of the analyzed system is

the fact that the algorithm can work in wide speed reference changes

## APPENDIX A (MOTOR DATA)

$P_N=1,1$  [kW];  $U_N=230/380$  [V];  $I_N=5,0/2,9$  [A];  $n_N=1380$  [r/min];  $f_N=50$  [Hz];  $p_b=2$ ;  $T_M=0.188$  [s]

$R_s$	$R_r$	$X_s$	$X_r$	$X_m$	Units
5,9	4,56	131,1	131,1	123,3	[ $\Omega$ ]
0,0776	0,06	1,725	1,725	1,6232	[p.u.]

## ACKNOWLEDGMENT

This research work was financed by the National Science Centre Poland under the project 2013/09/B/ST7/04199 (2014–2017).

## REFERENCES

- [1] F. Zidani, D. Diallo, M. E. H. Benbouzid, and E. Berthelot, "Diagnosis of speed sensor failure in induction motor drive," in *Proceedings book of the 2007 IEEE International Electric Machines and Drives Conference*, (Antalya), pp. 1680–1684, May 2007.
- [2] A. Adouni, M. B. Hamed, A. Flah, and L. Sbata, "Sensor and actuator fault detection and isolation based on artificial neural networks and fuzzy logic applied on induction motor," in *Proceedings book of the 2013 International Conference on Control, Decision and Information Technologies (CoDIT)*, (Hammamet, Tunisia), pp. 917–922, May 2013.
- [3] A. Bernieri, G. Betta, and A. P. a C. Sansone, "A neural network approach to instrument fault detection and isolation," *IEEE Transactions on Instrumentation and Measurement*, vol. 44, no. 3, pp. 747–750, 1995.
- [4] K. S. Lee and J. S. Ryu, "Instrument fault detection and compensation scheme for direct torque controlled induction motor drives," *IEE Proceedings - Control Theory and Applications*, vol. 150, no. 4, pp. 376–382, 2003.
- [5] S. Fan and J. Zou, "Sensor fault detection and fault tolerant control of induction motor drivers for electric vehicles," in *Proceedings book of the 2012 7th International Power Electronics and Motion Control Conference (IPEMC)*, (Harbin, China), pp. 1306–1309, June 2012.
- [6] M. Artioli, G. A. Capolino, F. Filippetti, and A. Yazidi, "A general purpose software for distance monitoring and diagnosis of electrical machines," in *Proceedings book of the 4th IEEE International Symposium on Diagnostics for Electric Machines, Power Electronics and Drives (SDEMPED)*, (Atlanta), pp. 272–276, August 2003.
- [7] R. M. Tallam, S. Lee, G. Stone, G. Kliman, T. H. J. Y. Yoo, and R. Harley, "A survey of methods for detection of stator-related faults in induction machines," *IEEE Transactions on Industry Application*, vol. 43, no. 4, pp. 920–933, 2007.
- [8] M. A. Rodriguez, A. Claudio, D. Theilliol, and L. G. Vela, "A new fault detection technique for igbt based on gate voltage monitoring," in *Proceedings book of the 2007 IEEE Power Electronics Specialists Conference*, (Orlando, FL), pp. 1001–1005, June 2007.
- [9] P. Sobanski, "Fuzzy-logic-based approach to voltage inverter fault diagnosis in induction motor drive," *Przeład Elektrotechniczny*, vol. 90, no. 6, pp. 149–153, 2014.
- [10] G. S. Buja and M. P. Kazmierkowski, "Direct torque control of pwm inverter-fed ac motors - a survey," *IEEE Transactions on Industrial Electronics*, vol. 51, no. 4, pp. 744–757, 2000.
- [11] T. Orlowska-Kowalska and M. Dybkowski, "Stator-current-based mras estimator for a wide range speed-sensorless induction-motor drive," *IEEE Transactions on Industrial Electronics*, vol. 57, no. 4, pp. 1296–1308, 2009.
- [12] L. Jiang, *Sensor fault detection and isolation using system dynamics identification techniques*. PhD thesis, The University of Michigan, 2011.
- [13] R. Isermann, *Fault Diagnosis Systems. An Introduction from Fault Detection to Fault Tolerance*. New York: Springer, 2006.
- [14] H. Berriri, M. W. Naouar, and I. Slama-Belkhdja, "Easy and fast sensor fault detection and isolation algorithm for electrical drives," *IEEE Transactions on Power Electronics*, vol. 27, no. 2, pp. 490–499, 2011.
- [15] K. S. Gaeid, "Fault tolerant control of induction motor," *Modern Applied Science*, vol. 5, no. 4, pp. 83–94, 2011.
- [16] M. Blanke, M. Kinnaert, and J. Lunze, *Diagnosis and Fault-Tolerant Control*. Berlin, Germany: Springer-Verlag, 2003.
- [17] M. E. Romero, M. M. Seron, and J. A. D. Dona, "Sensor fault-tolerant vector control of induction motors," *IET Control Theory and Applications*, vol. 4, no. 9, pp. 1751–1724, 2010.
- [18] J. Jiang and Y. Xiang, "Fault-tolerant control systems: A comparative study between active and passive approaches," *Annual Reviews in Control*, vol. 36, no. 1, pp. 60–72, 2012.
- [19] F. W. Fuchs, "Some diagnosis methods for voltage source inverters in variable speed drives with induction machines - a survey," in *Proceedings book of the 29th Annual Conference of the IEEE Industrial Electronics Society, 2003. IECON '03*, (USA), pp. 1378–1385, November 2003.
- [20] G. Betta and A. Pietrosanto, "Instrument fault detection and isolation: state of the art and new research trends," *IEEE Transactions on Instrumentation and Measurement*, vol. 49, no. 1, pp. 100–107, 2000.
- [21] P. Serkies and K. Szabat, "Predictive position control of the induction two-mass system drive," in *Proceedings book of the 23rd International Symposium on Industrial Electronics (ISIE)*, (Instanbul), pp. 871–876, June 2014.
- [22] H. Aradhye, "Sensor fault detection, isolation, and accommodation using neural networks, fuzzy logic and bayesian belief networks," Master's thesis, University of New Mexico, 2002.

- [23] S. Alag, A. M. Agogino, and M. Morjaria, "A methodology for intelligent sensor measurement, validation, fusion, and fault detection for equipment monitoring and diagnostics," *Artificial Intelligence for Engineering Design, Analysis and Manufacturing*, vol. 15, no. 4, pp. 307–320, 2001.
- [24] P. Vas, *Artificial-intelligence-based electrical machines and drives*. Oxford: Oxford University Press, 1999.



**Kamil Klimkowski** received the M.Sc. degree from the Electrical Engineering Faculty, Wrocław University of Technology, Wrocław, Poland, in 2013. Since 2014, he has been a member of the academic staff with the Electrical Drives Control, Institute of Electrical Machines, Drives and Measurements, Wrocław University of Technology. His main field of interest are the measurement sensors fault tolerant control methods for induction motor drives.



**Mateusz Dybkowski** received the Ph.D. and D.Sc. degrees from Wrocław University of Technology, Wrocław, Poland, in 2008 and 2014, respectively. Since 2008, he has been a member of the academic staff with the Electrical Drives Control, Institute of Electrical Machines, Drives and Measurements, Wrocław University of Technology. His main field of interest is the induction motor drive control and state variable estimations, control theory applications in electrical drives, digital signal processors, and field-programmable gate array applications.

#### AUTHORS' ADDRESSES

**Kamil Klimkowski, M.Sc.**  
**Mateusz Dybkowski, Ph.D., D.Sc.**  
**Department of Electrical Machines, Drives and Measurements,**  
**Wrocław University of Science and Technology,**  
**ul. Smoluchowskiego 19, 50-372 Wrocław, Poland,**  
**Phone: +48 71 320 34 67,**  
**Fax: +48 71 320 34 67,**  
**email: kamil.klimkowski@pwr.edu.pl,**  
**mateusz.dybkowski@pwr.edu.pl**

Received: 2016-01-11

Accepted: 2016-05-11